PHYSICAL REVIEW B **72**, 020408(R) (2005)

Orbital order in vanadium spinels

S. Di Matteo,[1,2] G. Jackeli,[3,*] and N. B. Perkins[1,4,5]
[1]*Laboratori Nazionali di Frascati INFN, via E. Fermi 40, C.P. 13, I-00044 Frascati (Roma), Italy*
[2]*Dipartimento di Fisica, Università di Roma III, via della Vasca Navale 84, I-00146 Roma, Italy*
[3]*Institute for Theoretical Physics, Ecole Polytechnique Fédérale de Lausanne, CH-1025, Lausanne, Switzerland*
[4]*Max-Planck-Institut för Physik komplexer Systeme, Nüthnitzer Str. 38 01187 Dresden, Germany*
[5]*Bogoliubov Laboratory of Theoretical Physics, JINR, 141980, Dubna, Russia*
(Received 2 May 2005; published 25 July 2005)

Motivated by recent theoretical and experimental controversy, we present a theoretical study to clarify the orbital symmetry of the ground state of vanadium spinel oxides AV_2O_4 (A=Zn, Mg, Cd). The study is based on an effective Hamiltonian with spin-orbital superexchange interaction and a local spin-orbit coupling term. We construct a classical phase diagram and prove the complex orbital nature of the ground state. Remarkably, with our analysis we predict correctly also the coherent tetragonal flattening of oxygen octahedra. Finally, through analytical considerations as well as numerical *ab initio* simulations, we propose how to detect the predicted complex orbital ordering through vanadium K-edge resonant x-ray scattering.

DOI: 10.1103/PhysRevB.72.020408 PACS number(s): 75.10.Jm, 75.30.Et

Vanadium and titanium spinels, AB_2O_4 (B=Ti^{3+} or V^{3+}), belong to a class of frustrated antiferromagnets where magnetic B ions are characterized by orbital degeneracy due to partial occupancy of t_{2g} orbitals ($n_{t_{2g}}=1$ for titanates and $n_{t_{2g}}=2$ for vanadates). Recently, these spinels were thoroughly studied from both experimental[1–3] and theoretical[4–6] points of view. While the ground state of Ti-based spinels can be explained in terms of orbitally driven superexchange interactions on the frustrated pyrochlore lattice,[6] the situation seems not so fluid for vanadium spinels, as two conflicting theoretical works appeared to explain their structural and magnetic properties.[4,5]

In AV_2O_4, magnetically active V^{3+}-ions form a pyrochlore lattice and are characterized by two $3d$ electrons in t_{2g}-orbitals, while A is a divalent ion like Cd^{2+}, Zn^{2+}, or Mg^{2+}. All compounds show qualitatively similar structural and magnetic behavior with a structural transition at a higher temperature T_S and an antiferromagnetic (AFM) transition at a slightly lower temperature T_N (Ref. 7). These findings have been interpreted by Tsunetsugu and Motome[4] as an interplay of $dd\sigma$ superexchange (SE) interaction and geometrical frustration: they showed that ordering of orbitals can partially remove magnetic frustration and explain the experimentally observed magnetic structure which is composed of AFM chains running in [110] and [$1\bar{1}0$] directions. The ground-state orbital ordering suggested in Ref. 4 consists of stacked ab planes with alternating d_{xz} and d_{yz} vanadium hole orbitals (hereafter referred to as ROO).

On the other side, Tchernyshyov[5] pointed out that the ground-state symmetry $I4_1/a$ of ROO solution seems at odds with x-ray and neutron diffraction data, indicating a $I4_1/amd$ space symmetry. Thus, he proposed a purely ionic model where spin-orbit (SO) coupling plays the major role and the V hole occupies [predetermining the sign of Jahn-Teller (JT) distortion] a complex linear combination of xz and yz orbitals: $(d_{xz}\pm id_{yz})/\sqrt{2}$. (We shall refer to this orbital order as COO).

Actually, the correct space group of the system is still elusive. The tetragonal $I4_1/amd$ space group was found in Ref. 1, while the authors of the neutron scattering experiment[2] supported ROO (thus, $I4_1/a$ space group) as more compatible with their findings. They found a clear signature of the one-dimensional (1D) character of spin fluctuations in the temperature range $T_N<T<T_S$, indicating a weak coupling between AFM chains. Based on this observation, and claiming that interchain coupling is much stronger for COO compared to ROO, they interpreted the experimental results in favor of the latter.

The aim of the present paper is to shed some light on this issue. To this end, we first link the two apparently unrelated pictures emerging from Refs. 4 and 5, and set them in a unique framework, by considering SE interaction and SO coupling on an equal footing and constructing a classical ground-state phase diagram. We demonstrate that the SO coupling favors the states with unquenched orbital momentum for any value of the coupling strength. We show that the only ground state which is compatible with the experimentally observed magnetic structure is the COO phase. This state is also characterized by a coherent tetragonal flattening of the oxygen octahedra along the same axis, as in real materials. Remarkably, this result is not predetermined by any *ad hoc* choice of JT interaction as was done in Refs. 4 and 5, but simply follows from our treatment of SE and SO interactions. We also evaluate the interchain spin couplings for both ROO and COO and find that they are comparable. Thus the experimental results of Ref. 2 cannot discriminate between the two types of orbital ordering. Finally, we suggest a possible key experiment to single out the proposed complex orbital states by means of magnetic resonant x-ray scattering (RXS). To this aim, we performed a formal analysis and an *ab initio* numerical simulation by means of the relativistic multiple scattering code in the FDMNES package.[8,9]

The effective Hamiltonian for AV_2O_4.—The model Hamiltonian consists of two parts, $H=H_{SE}+H_{SO}$. The first term represents the superexchange interaction between vanadium ions and the second term stands for the local spin-orbit coupling. First we discuss H_{SE}. The insulating phase of AV_2O_4 is of Mott-Hubbard type and the SE interaction can

be described by the Kugel-Khomskii model.[10] We borrow the SE Hamiltonian for V^{3+} ions, with threefold degenerate t_{2g} orbitals and spin $S=1$ from Ref. 11, to which we refer for technical aspects, and specialize it to our case. Hund's exchange, $J_H \simeq 0.68$ eV, and Coulomb on-site repulsion (same orbital), $U_1 \simeq 6.0$ eV, are taken from spectroscopy data.[12] For future convenience, we introduce the small parameter $\eta = J_H/U_1 \simeq 0.11$. Tight-binding fit to linear-augmented plane-wave calculations[13] shows that dominant overlap integrals are of σ type with $t = 3/4 t_{dd\sigma} = -0.24$ eV (Ref. 14). For this reason, we consider only nearest-neighbor (NN) hopping integrals of $dd\sigma$ kind on the pyrochlore lattice, as in Refs. 4 and 6. The $dd\sigma$ overlap in the $\alpha\beta$ plane ($\alpha\beta = xz, yz, xy$) connects only the corresponding orbitals of the same $\alpha\beta$ type. Thus, orbital operators are Ising-like and their contribution can be expressed simply in terms of projectors $P_{i,\alpha\beta}$ onto the occupied orbital state $\alpha\beta$ at site i, which are equal to 1 when the $\alpha\beta$ orbital is filled, or to 0 when it is empty. We finally get: $H_{\rm SE} = \frac{1}{2}\Sigma_{ij} H_{ij}$, where

$$H_{ij} = -[J_0 \vec{S}_i \cdot \vec{S}_j + J_1] O_{ij} - J_2 [1 - \vec{S}_i \cdot \vec{S}_j] \bar{O}_{ij} \qquad (1)$$

is the energy of bond ij. The orbital contributions O_{ij} and $\bar{O}_{ij}$ along the bond ij in the $\alpha\beta$ plane are given by: $O_{ij} = P_{i,\alpha\beta}(1 - P_{j,\alpha\beta}) + P_{j,\alpha\beta}(1 - P_{i,\alpha\beta})$ and $\bar{O}_{ij} = P_{i,\alpha\beta} P_{j,\alpha\beta}$. We defined: $J_0 = \eta J/[1-3\eta]$, $J_1 = J[1-\eta]/[1-3\eta]$, $J_2 = J[1+\eta]/[1+2\eta]$, and the inequality $J_0 < J_2 < J_1$ holds. The overall energy scale is $J = t_{dd\sigma}^2/U_1 \simeq 9.6$ meV.

The remaining local part of the effective Hamiltonian describes the relativistic spin-orbit coupling at each vanadium ion. We adopt the usual representation of effective $\vec{L}' = 1$ orbital angular momentum for t_{2g} electrons,[15] with $\hat{L}'_z |xy\rangle = 0$, and $\hat{L}'_z |xz \pm iyz\rangle/\sqrt{2} = \pm |xz \pm iyz\rangle/\sqrt{2}$. The true angular momentum $\vec{L}$ is related to the effective one by $\vec{L} \simeq -\vec{L}'$. With this notation $H_{\rm SO}$ can be written as: $H_{\rm SO} = -\lambda \Sigma_i \vec{L}'_i \cdot \vec{S}_i$, with $\lambda > 0$.

Real orbital configuration.—We first consider the states when only real orbitals are occupied. The orbital angular momentum is quenched and the local spin-orbit coupling is inactive. Such orbital patterns are eigenstates of the orbital part of $H_{\rm SE}$. This allows to classify all possible interacting bonds ij in $\alpha\beta$ planes in two categories: (i) weakly ferromagnetic (FM) b_1 bond, when only one of the two sites has an $\alpha\beta$ electron (O_{ij} contribution); and (ii) strongly AFM b_2 bond with both i and j ions occupied by $\alpha\beta$ electrons ($\bar{O}_{ij}$ contribution). There are also noninteracting bonds when neither i nor j have an $\alpha\beta$ orbital occupied. As we are interested in magnetic configurations of the whole pyrochlore lattice, in the following we limit our considerations to classical spins. The exchange coupling on b_1 bonds is given by $H_{b_1} = -J_0 \vec{S}_i \cdot \vec{S}_j - J_1$, with maximum FM energy gain: $E_{b_1} = J_0 + J_1$. For $\eta = 0$ the bond is nonmagnetic and $E_{b_1} = J$. The exchange coupling of b_2 bonds is given by $H_{b_2} = -J_2(1 - \vec{S}_i \cdot \vec{S}_j)$, and the maximum (AFM) energy gain is equal to $E_{b_2} = 2J_2$. For future convenience we point out that $E_{b_2} = 2E_{b_1}$ for $\eta = 0$, while $E_{b_2} < 2E_{b_1}$ for any finite η.

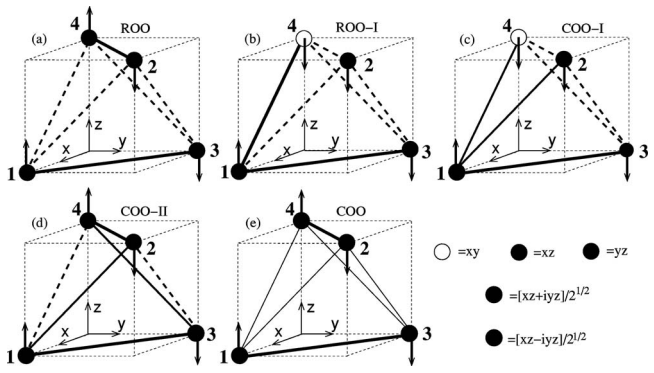

FIG. 1. Orbital, spin, and bond arrangements on a tetrahedron. (a), (b), (c), (d), and (e), respectively, correspond to ROO, ROO-I, COO-I, COO-II, and COO phases discussed in the text. Hole orbitals are shown. The solid (dashed) lines stand for AFM (FM) bonds. The thicker the line is, the stronger is the coupling on the bond.

In order to identify the lowest-energy state in the lattice, we introduce the operators $N^T_{b_1} = \Sigma'_{\langle ij \rangle} O_{ij}$ and $N^T_{b_2} = \Sigma'_{\langle ij \rangle} \bar{O}_{ij}$ that count the number of interacting b_1 and b_2 bonds on a tetrahedron. Using the identity for projectors $P_{i,xy} + P_{i,xz} + P_{i,yz} = 2$ (as there are two electrons occupying different orbitals at each site), one obtains $N^T_{b_1} + 2N^T_{b_2} = 8$. Rewriting this constraint in terms of energies of interacting b_1 and b_2 bonds, one finds that the energy gain per tetrahedron for $\eta = 0$ is always equal to $JN^T_{b_1} + 2JN^T_{b_2} = 8J$. Therefore, for $\eta = 0$, all real orbital patterns are degenerate.[16] However, as with increasing η the energy gain on b_2 bond decreases, while that on b_1 increases, and therefore the degeneracy is lifted. Thus, the lowest-energy configuration is the one with the maximum number of b_1 bonds per tetrahedron, which is $N^T_{b_1} = 4$ (recall that $N^T_{b_1} + N^T_{b_2} \leq 6$—the total number of bonds on a tetrahedron).

There are two topologically different tetrahedral configurations with $N^T_{b_1} = 4$ [see Figs. 1(a) and 1(b)]. In the case of ROO [Fig. 1(a)] there are two strongly AFM b_2 bonds located on opposite edges and coupled through weakly FM ($J' = -J_0$), frustrated b_1-bond interactions. When all tetrahedra are of ROO type, the average energy per site is $E_{\rm ROO} = -2J_1 - 2J_2$. The magnetic structure can be viewed as a collection of AFM chains running in [110] and $[1\bar{1}0]$ directions, coupled through frustrated interchain interaction J'. At the classical level the chains are decoupled from each other.

In the configuration ROO-I, the two strong AFM bonds share a corner and not all b_1 bonds are frustrated [Fig. 1(b)]. The spins of each tetrahedron form a fully collinear up-up-up-down (*uuud*) state with a finite magnetic moment equal to 1/2 of saturation value. The energy of this state $E_{\rm ROO-I} = -J_0 - 2J_1 - 2J_2$ is the lowest among those with quenched angular momentum. Thus, the ROO-I phase is the ground-state solution when $\lambda = 0$. However, it is at odds with experiments in both magnetic structure and JT distortion. In fact, the latter should have the same local axis at all sites, while this is not the case for the ROO-I phase. Notice again that in Ref. 4 the ROO ground state was found because JT coupling with only tetragonal distortion in the z direction was prein-

troduced. However, the inclusion of a local JT coupling with cubic symmetry will not affect the above results, as each state from the manifold would gain the same amount of JT energy by an elongation of each VO_6 octahedron along the local tetragonal axis.[10]

Complex orbital configuration.—Now consider the orbital configuration shown in Fig. 1(c) (COO-I), obtained from ROO-I by replacing a yz hole with $[xz+iyz]/\sqrt{2}$ at site 1. This site now carries angular momentum $L_z'=1$ and gains the SO energy λ. The spin couplings on bonds 1-2 and 1-4 are obtained by replacing orbital bond operators $O_{12(4)}$ and $\widetilde{O}_{12(4)}$ by their expectation values $\langle O_{12(4)}\rangle=\langle\widetilde{O}_{12(4)}\rangle=1/2$. This leads to the spin SE Hamiltonian $H_{12(4)}=[-J_1-J_2+(J_2-J_0)\vec{S}_1\cdot\vec{S}_{2(4)}]/2$, with AFM coupling $[J_2-J_0]/2>0$. Its ground-state energy is $E_{\text{COO-I}}=-J_0-2J_1-2J_2-\lambda/4$, which is lower than the lowest energy for real orbital patterns (ROO-I discussed above). Therefore, for any finite value of λ the states with quenched angular momentum are unstable with respect to those with unquenched L_z'. We can further construct the states with complex orbitals classifying them by the number of sites with nonzero L_z' per tetrahedron. The state with two complex sites [state COO-II, shown in Fig. 2(d)] has an average energy per site given by $E_{\text{COO-II}}=-3J_2-J_1-\lambda/2$. It is lower than the energy of COO-I for $\lambda>4[J_1-J_2+J_0]\sim 8\eta$. The magnetic order for such an OO can be regraded as a quasi-two-dimensional AFM pattern, formed by strong bonds [see the path 1-2-4-3-1 in Fig. 1(d)], with weak FM interaction along diagonals (bonds 1-4 and 2-3). The configuration with three complex sites has never the lowest energy. When all four sites carry nonzero L_z' [state COO, shown in Fig. 1(e)], the ground-state energy is $E_{\text{COO}}=-\frac{1}{2}[5J_2+2J_1]-\lambda$. The tetrahedron is characterized by two strong AFM b_2 bonds (2-4 and 1-3) and the lattice magnetic structure is given by 1D AFM chains running in [110] and $[1\bar{1}0]$ directions. The interchain coupling is frustrated and weakly AFM, with $J'=\frac{1}{4}[J_2-2J_0]$, contrary to the ROO phase whose $J'=-J_0$ is FM. Its strength is practically the same for both COO and ROO. For example, for $\eta=0.12$, $|J'|=0.14J$ for ROO and $|J'|=0.16J$ for COO. Therefore, in both cases the magnetic network is quasi-one-dimensional and the experimental results of Ref. 2 cannot rule out one or the other, as we have already outlined. Notice that the frustration of COO phase is much weaker than ROO phases, as the spin direction is fixed along the z axis by SO coupling and the degeneracy of the ground state is discrete as discussed in Ref. 5.

In Fig. 2 the ground-state phase diagram is shown in terms of the two dimensionless parameters $\widetilde{\lambda}=\lambda/J$ and η. The shaded rectangle represents the domain of realistic values for parameters: $\eta=0.8$–0.12 (Refs. 4 and 12), and $\lambda=13$–20 meV ($\widetilde{\lambda}=1.35$–2.08) (Ref. 5 and 17). Interestingly, if the system was close to the phase boundary, the application of an external magnetic field might induce the transition from COO, with zero magnetization, to COO-I, with a finite magnetic moment. The value of the field depends on how far from the phase boundary actual parameters locate the system. For the parameters within the shaded rectangle in Fig. 2

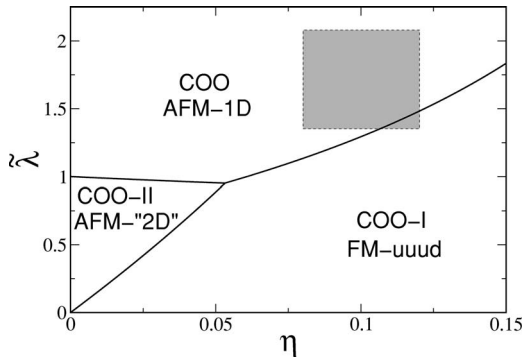

FIG. 2. Classical phase diagram of $H_{\text{SE}}+H_{\text{SO}}$ in $(\widetilde{\lambda},\eta)$ plane. The shaded rectangle denotes the domain of possible values of parameters.

the maximal value of the critical field is estimated to be $H_c\simeq 86\ T$. The magnetic-field experiment can be an interesting test of the phase diagram presented here.

To conclude the above consideration, we note that among ground states appearing in the phase diagram, only COO is compatible with the experimentally observed AFM structure. This type of orbital ordering also implies the coherent flattening of VO_6 octahedra along a unique axis leading to the experimentally observed tetragonal distortion. In what follows, we discuss a key experiment that we believe can give an unambiguous way to detect the suggested ground-state orbital order.

Experimental detection of COO phase.—An effective way to unravel the question of the orbital symmetry, both below T_N and between T_N and T_S, is by means of V K-edge RXS, where one is sensitive to the on-site value of L_z, as the local transition amplitudes are added with a phase factor that compensates the vanishing effect due to the global symmetry.[18] The elastic scattering amplitude is $A(\vec{Q},\omega)=\Sigma_j e^{i\vec{Q}\cdot\vec{\rho}_j}f_j(\omega)$, where $\vec{Q}$ is the momentum transfer in the scattering process, $\hbar\omega$ the photon energy, ρ_j the atomic positions in the unit cell, and the sum is over the eight atoms in the tetragonal cell. The atomic scattering factors (ASF), $f_j(\omega)$, is a second-order process in the electron-radiation interaction, given by (in the dipole approximation and atomic units)[19]

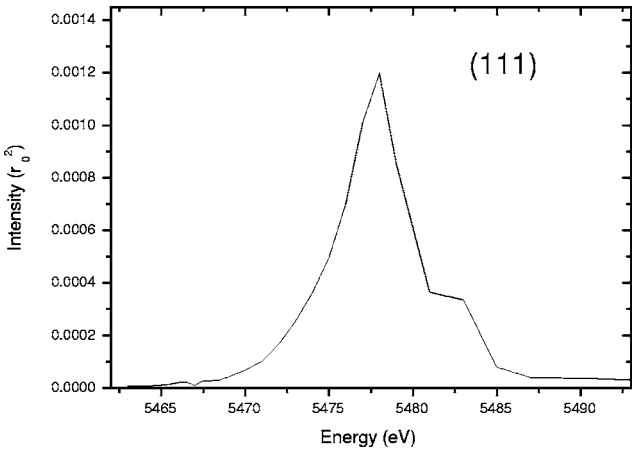

FIG. 3. Magnetic RXS at $(111)_{\sigma\pi}$ reflection for CdV_2O_4.

$$f_j(\omega) = (\hbar\omega)^2 \sum_n \frac{\langle \Psi_0^{(j)} | \hat{\epsilon}_s^* \cdot \vec{r} | \Psi_n^{(j)} \rangle \langle \Psi_n^{(j)} | \hat{\epsilon}_i \cdot \vec{r} | \Psi_0^{(j)} \rangle}{\hbar\omega - (E_n - E_0) - i\Gamma_n}, \quad (2)$$

where $|\Psi_0^{(j)}\rangle (|\Psi_n^{(j)}\rangle)$ is the ground (excited) state, with the origin taken on the jth scattering atom, and E_0 (E_n) is its energy; Γ_n takes into account the finite lifetime of the excited states, $\vec{\epsilon}_{i(s)}$ is the incident (scattered) polarizations, and $\vec{r}$ is the coordinate of the electron in the reference frame of the resonant ion. In the COO phase the space group is $I4_1/amd$, and we can write the structure factor in terms of the ASF of one single ion, through the symmetry operators $\hat{C}_{2z}$ and $\hat{C}_{4z}^{\pm}$ (twofold and fourfold rotation around the c axis) and $\hat{T}$ (time reversal): $S(\vec{Q}) = [1 + (-)^{h+k+l}\hat{T}][1 + (-)^{h+l}\hat{C}_{2z} + i^{h-k+l}\hat{C}_{4z}^{+} + i^{h+k-l}\hat{C}_{4z}^{-}]f_1$. For the $I4_1/a$ space group, induced by the reduced symmetry of the ROO phase, we get: $S(\vec{Q}) = [1 + (-)^{h+k+l}\hat{T}][1 + (-)^{h+l}\hat{C}_{2z} + i^{-h+k+l}\hat{C}_{4z}^{+} + i^{-h-k-l}\hat{C}_{4z}^{-}]f_1$. Therefore, for $h+k+l=$odd, both signals are proportional to $(1-\hat{T})$. As K-edge magnetic signals are a signature of nonzero orbital angular momentum, we can use V K-edge RXS to discriminate between the ROO phase, where no signal is expected, and the COO phase, where the signal is proportional to L_z (Ref. 9).

We have then performed a numerical simulation to estimate the order of magnitude of this signal for complex orbital occupancy with the relativistic multiple scattering code in the FDMNES package.[8,9] Results are shown in Fig. 3 for the (111) reflection in CdV_2O_4 (structural data were taken from Ref. 1). The incoming polarization is directed along one of a, b axes, where the intensity is the highest. The signal is of the order of $10^{-3}r_0^2$ at dipolar energies (r_0 is the classical electron radius), which is well within the present capabilities of third generation x-ray sources: this is a key experiment to choose the ground state in vanadate spinels. Probably a detectable signal could be obtained also through nonresonant magnetic x-ray scattering, thus allowing a quantitative measurement of L_z.

*Also at: E. Andronikashvili Institute of Physics, Georgian Academy of Sciences, Tbilisi, Georgia.

[1] M. Onoda, J. Hasegawa, J. Phys.: Condens. Matter **15**, L95 (2003); M. Reehuis *et al.*, Eur. Phys. J. B **35**, 311 (2003).

[2] S.-H. Lee *et al.*, Phys. Rev. Lett. **93**, 156407 (2004).

[3] M. Schmidt *et al.*, Phys. Rev. Lett. **92**, 056402 (2004).

[4] H. Tsunetsugu and Y. Motome, Phys. Rev. B **68**, 060405(R) (2003); Y. Motome and H. Tsunetsugu, *ibid.* **70**, 184427 (2004).

[5] O. Tchernyshyov, Phys. Rev. Lett. **93**, 157206 (2004).

[6] S. Di Matteo, G. Jackeli, C. Lacroix, and N. B. Perkins, Phys. Rev. Lett. **93**, 077208 (2004); S. Di Matteo, G. Jackeli, and N. B. Perkins, Phys. Rev. A **71**, 023610 (2005).

[7] Y. Ueda *et al.*, J. Phys. Soc. Jpn. **66**, 778 (1997).

[8] Y. Joly, Phys. Rev. B **63**, 125120 (2001).

[9] Y. Joly, S. Di Matteo, and C. R. Natoli, Phys. Rev. B **69**, 224401 (2004).

[10] K. I. Kugel and D. I. Khomskii, Usp. Fiz. Nauk **136**, 621 (1982) [Sov. Phys. Usp. **25**, 231 (1982)].

[11] S. Di Matteo, N. B. Perkins, and C. R. Natoli, Phys. Rev. B **65**, 054413 (2002).

[12] T. Mizokawa and A. Fujimori, Phys. Rev. B **54**, 5368 (1996).

[13] J. Matsuno, A. Fujimori, and L. F. Mattheiss, Phys. Rev. B **60**, 1607 (1999).

[14] The value $t_{dd\sigma} = -0.425$ eV given in Ref. 13 has to be scaled by the ratio of the fifth power of the relative V-V distance, which is 3.07 Å in, e.g., CdV_2O_4 (Ref. 1) and 2.91 Å in LiV_2O_4, used in Ref. 13.

[15] C. J. Ballhausen, *Introduction to Ligand Field Theory* (McGraw-Hill, NewYork, 1962), p. 89.

[16] We exclude the orbital patterns that generate frustrated spin-exchange paths and thus higher energy states.

[17] A. Abragam and B. Bleaney, *Introduction to Ligand Field Theory* (Clarendon, Oxford, 1970).

[18] Notice that a simple circular dichroism in absorption, as suggested in Ref. 4, is uneffective, as the average value of L_z over the unit cell is zero.

[19] M. Blume, J. Appl. Phys. **57**, 3615 (1985).